Interactive life-history traits predict sensitivity of plants and animals to temporal autocorrelation

Paniw, Maria ; Ozgul, Arpat ; Salguero-Gómez, Roberto

Abstract: Temporal autocorrelation in demographic processes is an important aspect of population dynamics, but a comprehensive examination of its effects on different life-history strategies is lacking. We use matrix population models from 454 plant and animal populations to simulate stochastic population growth rates (log s) under different temporal autocorrelations in demographic rates, using simulated and observed covariation among rates. We then test for differences in sensitivities, or changes of log s to changes in autocorrelation among two major axes of life-history strategies, obtained from phylogenetically informed principal component analysis: the fast-slow and reproductive-strategy continua. Fast life histories exhibit highest sensitivities to simulated autocorrelation in demographic rates across reproductive strategies. Slow life histories are less sensitive to temporal autocorrelation, but their sensitivities increase among highly iteroparous species. We provide cross-taxonomic evidence that changes in the autocorrelation of environmental variation may affect a wide range of species, depending on complex interactions of life-history strategies.

DOI: https://doi.org/10.1111/ele.12892

Interactive life-history traits predict sensitivity of plants and animals to temporal autocorrelation

A manuscript for consideration for publication in *Ecology Letters*

Maria Paniw[1,2*], Arpat Ozgul[1], Roberto Salguero-Gómez[3,4,5,6]

[1] Department of Evolutionary Biology and Environmental Studies, University of Zurich, Zurich 8057, Switzerland

[2] Department Biology, University of Cadiz, Puerto Real 11510, Spain

[3] Department of Zoology, Oxford University, New Radcliffe House, Radcliffe Observatory Quarter, Woodstock Rd, Oxford OX2 6GG, UK

[4] Department of Animal & Plant Sciences, University of Sheffield, Alfred Denny Building, Western Bank, Sheffield, S10 2TN. UK.

[5] Centre for Biodiversity and Conservation Science, University of Queensland, St Lucia 4071 QLD, Australia

[6] Evolutionary Demography Laboratory, Max Plank Institute for Demographic Research, Rostock 18057, Germany

[*]Corresponding author: Tel.: +41-(0)-4463-54912; email: maria.paniw@ieu.uzh.ch; ORCID ID: 0000-0002-1949-4448

Running title**:** Demography in autocorrelated environments

Statement of authorship: RSG performed phylogenetic analyses, MP performed modeling work and main analyses, with modeling framework on life-history traits developed by RSG and trade-off framework developed by AO, RSG, and MP. MP wrote the first draft of the manuscript, and all authors contributed substantially to revisions.

Data accessibility statement: All authors confirm that the data supporting the results are archived on Dryad and the data DOI is included at the end of the article. Matrix population models are available at www.compadre-db.org.

Keywords: environmental variation, fast-slow continuum, life-history strategy, matrix population model, multivariate analysis, population projections, reproductive strategy, seed dormancy, vital rates.

Word count: 150 abstract, 4996 main text; 62 References, 1 Table, 4 Figures

ABSTRACT

Temporal autocorrelation in demographic processes is an important aspect of population dynamics, but a comprehensive examination of its effects on different life-history strategies is lacking. We use matrix populations models from 454 plant and animal populations to simulate stochastic population growth rates ($\log \lambda_s$) under different temporal autocorrelations in demographic rates**,** using simulated and observed covariation among rates. We then test for differences in sensitivities, or changes, of $\log \lambda_s$ to changes in autocorrelation among two major axes of life-history strategies, obtained from phylogenetically-informed principal component analysis: the fast-slow and reproductive-strategy continua. Fast life histories exhibit highest sensitivities to simulated autocorrelation in demographic rates across reproductive strategies. Slow life histories are less sensitive to temporal autocorrelation, but their sensitivities increase among highly iteroparous species. We provide cross-taxonomic evidence that changes in the autocorrelation of environmental variation may affect a wide range of species, depending on complex interactions of life-history strategies.

INTRODUCTION

Most natural populations are exerted to environmental stochasticity (Tuljapurkar 1990; Boyce *et al*. 2006; Morris *et al*. 2008). Environmental fluctuations typically cause temporal variation in vital rates of individuals (*i.e*., survival, growth, and reproduction)**,** and the effects of such variation on population dynamics have been assessed in a number of theoretical and empirical studies using population models (Tuljapurkar 1990; reviewed in Ehrlén *et al*. 2016). However, temporal variation in environmental conditions has most often been modeled as independent and identically distributed (*i.i.d.*; e.g., Cohen 1979; Buckley *et al*. 2010), which assumes an

unrealistic lack of temporal autocorrelation in environmental fluctuations (Halley & Inchausti 2004; Ruokolainen *et al*. 2009).

A better understanding of how autocorrelated environmental perturbations of vital rates may determine current population dynamics is critical for eco-evolutionary questions and conservation management (Tuljapurkar 1982; Metcalf & Koons 2007; Ruokolainen *et al*. 2009; Smallegange *et al*. 2014). Temporally autocorrelated vital-rate variation may be an adaptation to non-independent phases of the environment, e.g., high recruitment cued to extreme weather or disturbances (Morris *et al*. 2006; Stige *et al*. 2007), favoring a selection of trait polymorphism (Orzack 1985; Uller 2008) and therefore increasing viability under a more variable climate (Nadeau *et al*. 2016). In particular, positive autocorrelation, which increases the likelihood of an environment remaining in one particular state (e.g., drought), may benefit species tolerant of climatic extremes and has been shown to increase invasiveness of aliens (Fey & Wiesczynski 2016). Therefore, trait selection and population dynamics in taxa sensitive to temporal autocorrelation may directly influence their potential to respond or adapt to environmental change (Morris *et al*. 2006; Koons *et al*. 2009; Engen *et al*. 2013; Nadeau *et al*. 2016).

Population-level responses to temporal autocorrelation are mediated by vital rates with the relatively strongest effect on the population growth rate (Franco & Silvertown 1996, 2004; Tuljapurkar & Haridas 2006). The relative effects of survival, growth, and reproduction on population dynamics meanwhile determine differences in life-history traits such as generation time and strategies, *i.e*., the combination of traits (Stearns 1992; Gaillard *et al*. 2016; Salguero-Gómez *et al*. 2016b). These interactions between vital rates, life histories, and environmental variation have been studied extensively in stochastic population analyses assuming i.i.d. Various studies have shown that long-lived species with *slow* life histories are generally buffered from

47 increased environmental variation (Morris *et al*. 2008, 2011; Sæther *et al*. 2013; but see
48 Jongejans *et al*. 2010; McDonald *et al*. 2017). Unlike long-lived species, short-lived species with
49 *fast* life histories, where reproduction contributes greatly to population dynamics, are expected to
50 show increasing fluctuations in population sizes with increasing environmental variation (Morris
51 *et al*. 2008; McDonald *et al*. 2017).

52 Although changes in the patterning of environmental noise may have significant
53 implications for population viability worldwide (Heino & Sabadell 2003; Ruokolainen *et al*.
54 2009; Fey & Wieczynski 2016), it remains largely unknown whether the proposed link between
55 life-history strategies and resilience to environmental fluctuations (Morris *et al*. 2008) holds in
56 autocorrelated environments. Theory predicts that populations that recover slowly from past
57 perturbations should be more sensitive to temporal autocorrelation than those that are more
58 resilient (Tuljapurkar & Haridas 2006). Low resilience has been shown for iteroparous, long-
59 lived plant species in constant environments (Salguero-Gómez *et al*. 2016b). However, the
60 limited empirical evidence shows weak support for increased sensitivities, or greater absolute
61 changes, of population growth rates of long-lived species to changes in temporal autocorrelation.
62 For example, studies on 11 terrestrial mammal species (Morris *et al*. 2011; Engen *et al*. 2013)
63 did not detect significant patterns, while others have concluded that long-lived species in
64 autocorrelated environments, both animals and plants, are buffered from environmental variation
65 regardless of reproductive strategy (e.g., Metcalf & Koons 2007; Morris *et al*. 2008).

66 To determine which life-history strategies are most sensitive to temporal autocorrelation,
67 we carried out stochastic simulations using matrix population models (MPMs hereafter) from
68 327 plant, three algae, and 126 animal populations. We ask whether species with slow life
69 histories show low sensitivities of stochastic population growth rates (log λ_s) to temporal

autocorrelation due to a low effect of environmental variation on these life histories (Morris *et al*. 2008). We also explore whether sensitivities differ between habitat types, as expected from the selection to distinct environmental noise patterns associated with them (e.g., Steele 1985; Vasseur & Yodzis 2004; Ruokolainen *et al*. 2009). We classify species according to main life-history strategies by performing a phylogenetically informed principle-component analysis (PCA) on life-history traits derived from MPMs. We then simulate stochastic population dynamics of each species' population by perturbing vital rates that define the MPMs based on serial autocorrelation in presumed environmental states. Our approach allows us to assess whether the effects of temporal autocorrelation on a given species' demography can be predicted from its life-history strategy, habitat type, or both.

MATERIALS AND METHODS

Matrix population models and vital rates

We used the COMPADRE Plant Matrix Database (Salguero-Gómez *et al*. 2015) and COMADRE Animal Matrix Database (Salguero-Gómez *et al*. 2016a) to obtain demographic data. These two databases provide high-quality MPMs representing a wide range of life histories, growth forms, and habitat types (Jones *et al*. 2014; Salguero-Gómez *et al*. 2016b). We limited our study to species that were studied in natural (*i.e*, unmanipulated) environments as we were interested in naturally-occurring patterns of life histories. For studies with > 2 years of data and/or > 1 population, we obtained the arithmetic element-by-element mean of all MPM entries to represent the average MPM across all studied years (Tuljapurkar & Haridas 2006). If several studies described the demography of one species, we kept MPMs of both studies only if they described distinct population dynamics from different ecoregions, e.g., species in the invaded vs.

93 natural range. Otherwise, we chose the study with greater temporal or spatial resolution. Using
94 these and other selection criteria (Appendix S1), we retained MPMs for 449 species and a total
95 of 454 populations, including 330 plant/red algae and 126 animal populations (Appendix S1). All
96 MPMs contained information on stage- or age-specific survival, transitions
97 (progression/retrogression), and reproduction (Fig. 1).

98 *Life-history patterns*

99 To characterize variation in life-history strategies among the populations studied, *i.e*., variation
100 in the pace of life (fast *vs*. slow) and reproductive strategy (spread of reproduction across the
101 lifespan), we derived five life-history traits from each MPM (Appendix S2). The chosen traits are
102 commonly used in comparative demographic studies for plants and animals (e.g., Franco &
103 Silvertown 1996; Tuljapurkar *et al*. 2009; Salguero-Gómez *et al*. 2016b): generation time (T),
104 age at sexual maturity (L_α), annual sexual reproduction (ϕ), degree of iteroparity (S), and net
105 reproductive rate (R_o). Details on the calculation of the traits can be found in Appendix S2 (see
106 also Caswell 2001).

107 To define main life-history strategies and relate them to sensitivities of log λ_s to temporal
108 autocorrelation in vital rates, we performed a varimax-rotated, phylogenetically-informed PCA
109 on the derived life-history traits (Revell 2012; Salguero-Gómez *et al*. 2016b). The traits were
110 log-transformed and scaled to $\mu = 0$ and SD = 1 to agree with PCA assumptions. To correct for
111 phylogenetic relatedness among species in the PCA, we constructed a species-level phylogenetic
112 tree coercing different populations of the same species as dichotomous branches at the five
113 species' tips. In the tree, branch length informed about phylogenetic relatedness (Appendix S2).
114 The phylogenetically informed PCA then linked the phylogeny to life-history traits via a

modified covariance matrix and estimated Pagel's λ, a scaling parameter for the phylogenetic correlation between species (Freckleton *et al*. 2002; for details see Appendix S2).

Defining environmental states

To incorporate temporal autocorrelation into stochastic simulations of population dynamics of the 454 populations, we defined a discrete Markov chain consisting of two states, (i) favorable or good environmental conditions and (ii) unfavorable or bad conditions. The transitions between the two states were defined using the transition matrix:

$$\begin{pmatrix} \mathrm{p}_g & \mathrm{p}_b \\ 1-\mathrm{p}_g & 1-\mathrm{p}_b \end{pmatrix}$$

Here, p_g and p_b are the probabilities of transitioning to the good environment at time *t*+1 when the environment was good or bad at *t*, respectively. These transitions can be derived from the long-term frequency of the good environment (*f*) and temporal autocorrelation, v_1 (Tuljapurkar & Haridas 2006), where $p_b = f(1 - v_1)$ and $p_g = (v_1 + p_b)$.

Linking vital rates to environmental states

For most populations (85 %) used in this study, < 5 annual transitions were recorded (Appendix S1). This may limit the reliability of estimates of vital-rate variability and in particular autocorrelation – both requiring long-term population time series (Jongejans *et al*. 2010; Engen *et al*. 2013; Metcalf *et al*. 2015). Therefore, while using real life histories described by various combinations of mean vital rates, we perturbed vital rates away from their means for all 454 MPMs based on biologically relevant assumptions of environmental variation and patterning (but see *Empirical analyses* for additional simulations using observed vital-rate covariation). At the same time, our approach assumes that (a) transition probabilities between environmental states

remain constant through time and (b) all vital rates potentially respond to changes in environmental conditions (*i.e.*, incomplete buffering), although these responses are constrained as detailed below.

To link vital rates to the good and bad environment, we derived above- and below-average distributions of each vital rate across populations using three different coefficients of variation (CV; Fig. 1). We determined a new average vital-rate value for good (bad) environments by increasing (decreasing) a given vital-rate value from the mean MPM as a function of the CV (Fig. 1; Appendix S3; Koons *et al*. 2008). For vital rates describing reproduction, the three raw CV values were used in simulations (see Appendix S3 for additional simulation using higher CV). Vital rates describing survival or stage/age transitions however, were assumed to have a binomial distribution and therefore a maximum bound on their variance and CV (CV_{max}; Morris & Doak 2004). We obtained new average values of these vital rates for good and bad states as a function of $CV \times CV_{max}$. This constraint prevented vital rates with high average values (e.g., adult survival in long-lived species) to vary more extremely between good and bad environmental states than vital rates with relatively lower average values, making simulations more biologically realistic (Koons *et al*. 2008; see Fig. S3.1 in Appendix S3 for distribution of vital rates across environmental states). Such extreme variation would otherwise occur when the CV used in simulations approached the maximum variance of binomial vital rates.

Using the new average vital-rate values for good and bad environments, we simulated 100 vital rates from the beta (for survival/transitions) and gamma (for reproduction) distributions for each environmental state, keeping the non-perturbed vital rates at their mean and therefore assuming no vital-rate covariation. We then assembled 100 MPMs per species and vital rate for

158 good and bad environments. Each of these 100 MPMs was picked at random during stochastic
159 simulations of population dynamics (Fig. 1).

160 *Stochastic simulations of population dynamics*

161 We performed one simulation run for each vital rate per MPM using two long-term frequencies
162 of the good environment (f = 0.35 and 0.65) × 3 autocorrelations (v_1 = -0.3, 0, and 0.3) × 3
163 degrees of vital-rate variation between good and bad environments (CV = 0.2, 0.5, and 0.8). For
164 each parameter combination, we obtained the stochastic population growth rate, log λ_s, by
165 projecting population dynamics for 500,000 time steps after discarding the initial 20,000
166 iterations (see Tuljapurkar *et al*. 2003). For each species, we repeated 50 simulation runs to
167 account for the stochastic process from which MPMs for good and bad environmental states
168 were assembled (sampling from beta and gamma distributions; Appendix S3). From all
169 simulations, we obtained the sensitivity of log λ_s to autocorrelation, $S^{v_1} = \frac{|\partial \log \lambda_s|}{|\partial v_1|}$, the absolute
170 changes in the stochastic population growth rate as autocorrelation changed from 0 to positive
171 (0.3) or negative (-0.3) (Fig. 1). We quantified changes in absolute terms to focus on the
172 magnitude of S^{v_1}.

173 *Sensitivities to temporal autocorrelation across life histories*

174 We used generalized additive models (GAMs) to correlate S^{v_1}, averaged across the 50
175 simulation runs, to simulation parameters (f and CV) and life histories (PCA axes) while
176 accounting for non-linear trends. We assumed a log-normal distribution of S^{v_1}, which provided a
177 better fit to the data than a normal distribution (Appendix S3), and chose the most parsimonious
178 models based on AIC scores (Akaike 1971). First, we quantified differences in S^{v_1} across f and
179 CV. For each combination of f and CV, we then modeled S^{v_1} across distinct vital rates perturbed

in simulations as a function of life-history strategies, *i.e.*, scores along the main PCA axes. To increase statistical power and facilitate comparisons across species, we grouped perturbed vital rates prior to modelling by

(i) assigning each stage/age class of an MPM to either the propagule, pre-reproductive, reproductive, or non-reproductive class (Appendix S1) and

(ii) summing S^{v_1} for survival, stage/age transitions, and reproduction within each class (Appendix S3).

When fitting GAMs, we excluded vital-rate classes (mostly non-reproductive class) that were present in < 20 % of populations (Appendix S3).

Lastly, to explore global trends in S^{v_1}, we modeled S^{v_1} across different vital-rate classes as a function of major habitat type. To allow for statistical comparisons, we summed S^{v_1} for survival, transitions (progression/retrogression), and reproduction for all stages/ages. Information on major habitat types was obtained from COMADRE and COMPADRE. We collapsed habitat types from the original 39 types to five: temperate, tropical & subtropical, arid, alpine & arctic, and aquatic (see Appendix S1). We accounted for the effect of MPM dimension and population on the variation in $S^{v_1}$by fitting the latter two as random effects in the GAMs (see Appendix S3 for discussion on the relevance of MPM dimension).

Empirical analyses

To test the robustness of simulating different CV against natural vital-rate variation, we extracted vital rates for a subset of 109 populations with at least three annual MPMs and used the observed vital-rate correlation to estimate population dynamics in good and bad environmental states (Appendix S4). That is, we assembled 1,000 MPMs for good and bad environments from a

multivariate vital-rate distribution, using copulas to combine marginal gamma (for reproduction) and beta (for survival/transitions) distributions based on vital-rate correlations (Koons *et al*., 2008; Jongejans *et al*. 2010; Appendix S4). Simulation and statistical analyses of S^{v_1} then followed the steps outlined above, although we collapsed the habitats to two categories, temperate (n = 63) and other (n = 46) to allow for statistical comparisons.

We used two approaches to test the robustness of simulating temporal autocorrelation. First, we compared our S^{v_1} obtained from simulations of temporal autocorrelation (for the subset of 109 species modeling observed vital-rate CV) with empirical evidence for the contribution of temporal autocorrelation to vital-rate variation. To obtain the latter, we identified 13 species where MPMs were available for ≥ 10 consecutive annual transitions within a given site. We then regressed all vital rates at time *t* against vital-rate values at *t*-1, fitting first-order autoregressive models using a quasi-binomial (for survival/transitions) and gamma (for reproduction) error distributions. Lastly, we correlated average deviance explained by the models across vital rates, a measure of the importance of temporal autocorrelation in explaining vital-rate variation, to S^{v_1}. Second, we compared our simulated S^{v_1} using the full set of 454 populations with published information, noting whether autocorrelated environmental variation was explicitly examined in previous studies, and whether it significantly affected stochastic population dynamics (Appendix S4).

RESULTS

Life-history patterns

The life histories of the 449 studied species (454 populations) were adequately captured by two main PCA axes that together explained 67 % of variation in key life-history traits (Fig. 2).

224 Following the Kaiser criterion (Appendix S2), we kept these first two PCA axes for subsequent
225 analyses, since their associated eigenvalues were > 1. PCA axis 1 largely captured the position of
226 the species' populations along the fast-slow continuum, with greatest positive loadings for age at
227 sexual maturity (L_o) and generation time (T), and negative loadings of annual sexual
228 reproduction (ϕ), depicting a tradeoff between survival and reproduction (Gaillard *et al*. 2016;
229 Salguero-Gómez *et al*. 2016b). PCA 2 largely captured variation in reproductive strategies, with
230 largest positive loadings corresponding to highly iteroparous (S) species with a high net
231 reproductive rate (R_o) and ϕ (Fig. 2). The positive loading of ϕ onto PCA 2 was explained by a
232 strong association between annual reproduction and iteroparity in plants (Salguero-Gómez *et al*.
233 2016b). When considering plants/algae and animals separately, ϕ loadings onto PCA 2 were
234 negligible for the latter (Figure S2.1), which is consistent with previous studies on animals
235 (reviewed in Gaillard *et al*. 2016). Similarly, R_o loaded onto PCA 1 due to the presence of long-
236 lived plants with high R_o in the data (Fig. 2; Fig. S2.1). Therefore, the fast-slow and
237 reproductive-strategies axes were not entirely represented by unique traits when considering both
238 plants and animals. The phylogenetic relationships of the examined species moderately shaped
239 their relative positioning along the life-history strategy space with Pagel's $\lambda = 0.61$ (±0.1 S.D.).

240 *Sensitivity to temporal autocorrelation across life histories*

241 The stochastic population growth rate, log λ_s, did not change significantly in magnitude when
242 positive (from 0 to 0.3) *vs*. negative (from 0 to -0.3) changes in temporal autocorrelation were
243 simulated (Fig. S3.5). Thus, here we present results of S^{ν_1}, the sensitivity of log λ_s to positive
244 perturbations of autocorrelation. S^{ν_1} increased > 10-fold as the coefficients of variation (CV)
245 used for perturbing vital rates increased from 0.2 to 0.8, but differed little among the two

246 frequencies of the good environmental state, f (Table 1; but see Appendix S3 for the strong effect
247 of f on log λ_s).

248 For the examined CV and f, a significant interaction between the fast-slow (PCA 1) and
249 reproductive-strategies (PCA 2) continua and vital-rate classes perturbed described S^{v_1} patterns
250 (Table 1; Fig. 3a). For most vital-rate classes, faster life histories showed high S^{v_1} across a wide
251 range of reproductive strategies. Highest S^{v_1} were found for pre-reproductive survival and
252 transitions (Table 1; Fig. 3a). Populations with slower life histories, on the other hand, showed
253 increased S^{v_1} only when they also had a high reproductive output (Fig. 3a). When including the
254 effect of habitat, populations were most sensitive to temporal autocorrelation when the
255 perturbations happened in survival (S) and transitions (T) rather than in reproduction (R) across
256 all habitats considered (Fig. 3b). Perturbations of the latter vital-rate class had the highest effect
257 in aquatic habitats. Removing outliers both in simulated S^{v_1} and PCA scores did not significantly
258 affect GAM relationships (Appendix S3).

259 *Empirical analyses*

260 The additional empirical analyses validated our simulations. S^{v_1} based on naturally observed
261 vital-rate covariation for 109 populations showed very similar patterns of variation along life-
262 history strategies and habitat types as S^{v_1} based on simulated CV (Table 1; Fig. 4a; Fig. S4.1). In
263 addition, S^{v_1} were significantly correlated (using a log scale; $R^2 = 0.63$; $p < 0.05$) with the
264 contribution of autocorrelation to observed vital-rate variance from 13 populations (Fig. 4b).
265 Lastly, we obtained significantly higher S^{v_1} for populations where previous studies included
266 temporal autocorrelation in stochastic population models than for populations modeled assuming
267 only i.i.d. environments ($t_{65} = 2.3$, $P = 0.01$; Fig. 4c; Appendix S4). However, the effects of

temporal autocorrelation on population dynamics have been assessed for only 8 % of the 454 populations simulated here and have been omitted for many species with high S^{ν_1}(Appendix S4). Our simulations indicate that approx. 44 % of populations affected by environmental variation may also be affected by changes in the patterning of environmental states (Fig. 4c; Appendix S4).

DISCUSSION

Identifying life-history strategies associated with high sensitivities of demographic processes to temporal autocorrelation may allow for a much-needed inference on species affected by predicted changes in the patterning of environmental noise (Heino & Sabadell 2003; Laakso *et al*. 2003; Engen *et al*. 2013). Using data on 454 naturally occurring plant/algae and animal populations (449 species), we provide global empirical evidence that the fast-slow continuum of life-history variation, interacting with a species' reproductive strategy, help predict the demographic vulnerability to temporal autocorrelation (Table S2.2). In addition, our results highlight that life-history responses to the temporal autocorrelation may be strongly mediated by vital rates and habitat types affected by changes in environmental patterning.

Although, generally, long-lived species have been predicted to be more sensitive to perturbations in population structure than short-lived species (Franco & Silvertown 2004; Salguero-Gómez *et al*. 2016b; but see Gamelon *et al*. 2014) and hence potentially to temporal autocorrelation (Tuljapurkar & Haridas 2006), our simulations indicate that most long-lived organisms are buffered not only against increases in vital-rate variation (e.g., Morris *et al*. 2008; Tuljapurkar *et al*. 2009; McDonald *et al*. 2017) but also against changes in its temporal patterning. Our results agree with theory showing a negative correlation between generation time and magnitude of the effect of serial vital-rate correlations on fitness in age-structured

291 populations (Tuljapurkar *et al*. 2009; Sæther *et al*. 2013). In empirical studies, low sensitivities to
292 both interannual vital-rate variation and temporal autocorrelation have been found for several
293 mammal species, e.g., *Brachyteles hypoxanthus* and *Gorilla beringei* (Morris *et al*. 2011; Engen
294 *et al*. 2013). Most of these species were located at the slow end of life-history strategies in our
295 analyses and exhibited, along with most long-lived aquatic (e.g., *Paramuricea clavata*) and tree
296 and herbaceous species (e.g., *Calocedrus decurrens*) low simulated sensitivities of their growth
297 rates to temporal autocorrelation (Fig. 2).

298 The low sensitivities of population growth rates to temporal autocorrelation in long-lived
299 species may be explained by vital-rate specific responses to changes in environmental patterning
300 (Ezard & Coulson 2010). Species with slow life histories are characterized by high juvenile and
301 adult survival (Franco & Silvertown 2004; Morris *et al*. 2008; Morris *et al*. 2011), which are
302 typically less affected by environmental variation (Morris & Doak 2004; McDonald *et al*. 2017)
303 or autocorrelation (Morris *et al*. 2008, 2011). Our simulations replicated such buffering by
304 constraining the variation in binomial vital rates by the maximum coefficients of variation
305 (CV_{max}; Morris & Doak 2004; Koons *et al*. 2008). Therefore, slow life histories vulnerable
306 largely to changes in adult survival, which varied little if the average value was high (Appendix
307 S3), responded overall weakly to changes in temporal autocorrelation. On the other hand,
308 perturbing adult survival resulted in highest sensitivities for populations where this vital rate
309 showed more variation but remained of relatively high importance for life-cycle dynamics, *i.e.*,
310 for shorter-lived semelparous species (Metcalf & Koons 2007). Similarly, some short-lived
311 species, such as the invasive plant *Brassica napus*, where annual reproduction dominates life-
312 cycle dynamics (Garnier *et al*. 2006), may be little affected by environmental patterning in
313 growth or survival (Fig. 4b). These patterns of vital-rate specific sensitivities remained when

omitting a maximum bound on vital-rate variation to allow for extreme life histories (Fig. S3.4 in Appendix S3; Jongejans *et al*. 2010; McDonald *et al*. 2017) or when increasing the CV in reproduction perturbations (Fig. S3.5 in Appendix S3). This indicates that our results were not an artifact of the CV used. Most importantly, our simulations highlight that interpreting a population's responses to temporal autocorrelation requires detailed knowledge of the variation in underlying vital rates (Morris & Doak 2004; Ezard & Coulson 2010).

In addition to its location along the fast-slow continuum, a species' reproductive strategy (Salguero-Gómez *et al*. 2016b; Salguero-Gómez 2017) was also critical to capture its sensitivity to temporal autocorrelation. In fact, some long-lived species showed relatively high sensitivities to temporal autocorrelation (Fig. 2). Most of these species were plants, for example the invasive big-sage (*Lantana camara*) or the tropical, seed-bank producing, tree *Ardisia elliptica*, and were characterized by relatively large net reproductive rates (R_0) and degree of iteroparity. These species explain the positive loading of R_0 onto the first life-history strategy axis, otherwise dominated by life span and total annual reproduction. They show that slow life histories may be highly susceptible to environmental patterning if they also spread their reproduction over many years (McDonald *et al*. 2017). Examples may include species that "track" changes in the environment by opportunistically recruiting in gap openings in forests or coral reefs. For such species, predictable, high-recruitment events, accompanied by relatively low survival of offspring, define population dynamics (Connell 1978; Metcalf *et al*. 2009). On the other hand, slow life histories with semelparous reproductive strategies have been shown to be buffered from changes in the patterning of environmental states (Metcalf & Koons 2007) and also exhibited lowest sensitivities in our simulations (Fig 3).

Aside from some slow life histories with a high reproductive mode, a large number of taxa with a short life span and high annual reproduction exhibited the highest simulated sensitivities to temporal autocorrelation. This was true across semelparous and iteroparous species. Short-lived aquatic, e.g., the clam *Mya arenaria*, and terrestrial animals, e.g., the rodent *Tamiasciurus hudsonicus*, many insect species, e.g., *Scolytus ventralis*, and numerous short-lived plants, particularly invasive ones, e.g., *Cirsium vulgare*, are highly sensitive to changes in vital rates other than adult survival and also exhibit high variability in these vital rates depending on the state of the environment (Meijden *et al*. 1992; Morris *et al*. 2008; Koons *et al*. 2009). For such taxa, assessing the patterning of environmental variation would likely greatly improve knowledge on population dynamics (Jongejans *et al*. 2010). However, such assessments are lacking, as quantified in a thorough literature review here (Appendix S4), particularly for aquatic species and insects.

A common life-cycle adaptation to track autocorrelated environmental variation, *e.g.*, to recruit only under favorable conditions, is dormancy (Cáceres 1997; Morris *et al*. 2006). Plant species with dormant propagule stages (seed banks), adapted to disturbance-prone habitats (Doak *et al*. 2002), exhibited the highest sensitivities of their growth rates to temporal autocorrelation (Fig. 2a). For species like *Mimulus lewisii* (Fig. 2b), whose populations are regularly exposed to flooding, changes in disturbance regimes and patterns of post-disturbance habitat succession may be detrimental to viability (Angert 2006; Turner 2010). In addition, propagation of many invasive plant species is aided by seed banks (Gioria *et al*. 2012). Such species, e.g., *Ardisia elliptica* or *Lantana camara*, exhibited high sensitivities to temporal autocorrelation, despite being relatively long-lived (Fig. 2). Although environmental patterning may be critical for plant invasion (Fey & Wiesczynski 2016), its importance was only considered in previous studies for

one out of ten invasive populations included in our analysis (Appendix S1). For animals, MPMs do not typically include dormant propagule stages (Salguero-Gómez *et al*. 2016), such as cysts or larvae in diapause (Cáceres 1997; Schiesari & O'Connor 2013). Such species may be particularly vulnerable to predicted changes in environmental condition or may constitute emerging pests (Cáceres 1997), and must therefore be the focus of more research.

In addition to species with dormant life cycles, habitat-specific population dynamics deserve a particular focus when assessing potential ecological impacts of global changes in environmental patterning. Our simulations show that sensitivities of stochastic growth rates to temporal autocorrelation differ between major habitat types, particularly when perturbing reproduction. For the latter, sensitivities for fast life histories were highest in aquatic habitats, although populations in aquatic habitats represent a narrow sample of the total life-history PCA space (Fig. 3). Differences in sensitivities to temporal autocorrelation between terrestrial and aquatic systems may be explained by the fact that the latter are more strongly (positively) autocorrelated and therefore predictable (Steele 1985; Cáceres 1997; Vasseur & Yodzis 2004). Therefore, species, such as the fish *Sardina pilchardus*, may exhibit strong responses when environmental patterns change, particularly due to anthropogenic influences (Ruokolainen *et al*. 2009). However, MPMs on aquatic species are still relatively scarce (Fig. 3b), and the effects of temporal autocorrelation on population dynamics in aquatic systems are rarely considered (Appendix S4). The same is true for arctic & alpine habitats, where climate change is predicted to have major effects on population dynamics (Post *et al*. 2009). At the same time, the relationship between the two major life-history axes and the sensitivity to temporal autocorrelation held in all habitats studied, indicating that future changes in the patterning of

environmental states may significantly affect species globally (Vasseur & Yodzis 2004; Turner 2010).

Our results are robust to the choice of CV when perturbing vital rates and are in agreement with previous empirical studies regarding the importance of temporal autocorrelation in population dynamics (Fig. 4; Appendix S4). However, five aspects need further attention. First, the MPMs that were available to us represent a biased subset of life histories, given the underrepresentation of certain habitat types and life cycle (Salguero-Gómez *et al*. 2015, 2016a). Our life-history framework must therefore be validated with future additions of little-studied taxa. Second, density dependence was not considered in our study but is known to interact with temporal autocorrelation to regulate population responses (Levine & Rees 2004; Greenman & Benton 2005; Engen *et al*. 2013). A recent study by Koons and colleagues (2016) incorporated population structure and density-dependence to assess differences in vital-rate variation among life-history strategies; future studies would benefit from applying this approach to serial vital-rate correlations. Third, our simulations of changes in environmental states may not have reflected complex processes such **as** habitat succession (e.g., Tuljapurkar & Haridas 2006). Fourth, we simulated autocorrelated changes in environmental states on an annual basis, potentially producing stronger effects for short-lived species simply due to the temporal scale used (Vasseur & Yodzis 2004; Stige *et al*. 2007). Lastly, our simulations of vital-rate variation omitted complex demographic processes such as strong buffering (no variation in vital rates among years; e.g., Morris *et al*. 2011) and nuances in covariation beyond the ones considered for the 109 species (Jongejans *et al*. 2010). Therefore, while we provide a robust general assessment of the role of autocorrelation across life histories and habitats, we acknowledge that a more detailed assessment must rely stronger on empirical data.

CONCLUSIONS

Temporal autocorrelation in demographic processes, historically rarely considered in demographic studies, may have strong effects, across habitats, on fast and slow life histories alike, depending on the reproductive strategy. Importantly, we found that taxa exhibiting highest sensitivities to temporal autocorrelation are also the ones least studied. With predicted global changes in environmental patterning, we argue that future demographic studies will only accurately predict important population processes such as viability or invasiveness if researchers explicitly consider the effects of these changes on key underlying demographic rates like survival, stage/age-specific transitions, and reproduction.

ACKNOWLEDGEMENTS

We thank H. Caswell, J.D. Lebreton, and S. Tuljapurkar for helpful suggestions on the characterization of life histories, Dr. Ezard and 2 anonymous reviewers for constructive criticism on earlier version of this work, and the Max Planck Institute for Demographic Research for support and open-access to COMPADRE & COMADRE. This study was partly financed by BREATHAL (CGL2011-28759/BOS; Spanish *Ministerio de Economía y Competitividad*). M.P. was supported by a FPI scholarship, a travel bursary granted by the Spanish *Ministerio de Economía y Competitividad,* and an ERC Starting Grant (#337785) to A.O. R.S.-G. was supported by the Australian Research Council (DE140100505) and NERC (R/142195-11-1).

REFERENCES

425 Akaike, H. (1971) Information theory and an extension of the maximum likelihood principle. In:
426 *2nd International Symposium on Information Theory*. Petrov, B.N. & Csaki, B.F. (eds.).
427 Academiai Kiado, Budapest, pp. 267-281.

428 Angert, A.L. (2006). Demography of central and marginal populations of monkeyflowers
429 (*Mimulus cardinalis* and *M. lewisii*). *Ecology*, **87**, 2014-2025.

430 Boyce, M.S., Haridas, C.V., Lee, C.T. & NCEAS Stochastic Demography Working Group.
431 (2006). Demography in an increasingly variable world. *Trends Ecol. Evol.,* **21**, 141-148.

432 Buckley, Y.M., Ramula, S., Blomberg, S.P., Burns, J.H., Crone, E.E., Ehrlén, J., *et al*. (2010).
433 Causes and consequences of variation in plant population growth rate: a synthesis of matrix
434 population models in a phylogenetic context. *Ecol. Lett.*, **13**, 1182-1197.

435 Cáceres, C.E. (1997). Dormancy in invertebrates. *Invertebr. Biol.,* **1**, 371-383.

436 Caswell, H. (2001). *Matrix Population Models: Construction, Analysis and Interpretation.* 2nd
437 ed. Sinauer Associates, Sunderland, US, pp. 722.

438 Cohen JE. (1979). Comparative statics and stochastic dynamics of age-structured populations.
439 *Theor. Popul. Biol.*, **16**, 159-171.

440 Connell, J.H. (1978). Diversity in tropical rain forests and coral reefs. *Science* **199**, 1302-1310.

441 Doak, D.F., Thomson, D. & Jules, E.S. (2002). Population viability analysis for plants:
442 understanding the demographic consequences of seed banks for population health. In: *Population*
443 *Viability Analysis*. Beissinger, S.R. & McCullough, D.R. (eds.). University of Chicago Press,
444 Chicago, Illinois, US, pp. 312-337.

445 Ehrlén, J., Morris, W.F., Euler, T. & Dahlgren, J.P. (2016). Advancing environmentally explicit
446 structured population models of plants. *J. Ecol.,* **104**, 292-305.

447 Engen, S., Sæther, B.E., Armitage, K.B., Blumstein, D.T., Clutton-Brock, T.H., Dobson, F.S., *et*
448 *al*. (2013). Estimating the effect of temporally autocorrelated environments on the demography
449 of density-independent age-structured populations. *Methods Ecol. Evol.,* **4**, 573-84.

450 Ezard, T.H. & Coulson, T. (2010). How sensitive are elasticities of long-run stochastic growth to
451 how environmental variability is modelled? *Ecol. Model*., 221, 191-200.

452 Fey, S.B. & Wieczynski, D.J. (2016). The temporal structure of the environment may influence
453 range expansions during climate warming. *Global Change Biol.*, **23**, 635-645.

454 Franco, M. & Silvertown, J. (1996). Life history variation in plants: an exploration of the fast-
455 slow continuum hypothesis. *Phil. Trans. R. Soc. B.*, **351**, 1341-1348.

456 Franco, M. & Silvertown, J. (2004). A comparative demography of plants based upon elasticities
457 of vital rates. *Ecology*, **85**, 531-538.

458 Freckleton, R.P., Harvey, P.H. & Pagel, M. (2002). Phylogenetic analysis and comparative data:
459 A test and review of evidence. *Am. Nat.,* **160**, 712–726.

460 Gaillard, J.M., Lemaître, J.F., Berger, V., Bonenfant, C., Devillard, S., Douhard, M., *et al*.
461 (2016). Life histories, axes of variation in. In: *Encyclopedia of Evolutionary Biology*, vol. 2.
462 Kliman, R.M. (ed.). Academic Press, Cambridge, Massachusetts, US, pp. 312–323.

463 Gamelon, M., Gimenez, O., Baubet, E., Coulson, T., Tuljapurkar, S. & Gaillard, J.M. (2014).
464 Influence of life-history tactics on transient dynamics: a comparative analysis across mammalian
465 populations. *Am. Nat.*, 184, 673-683.

Garnier, A. & Lecomte, J. (2006). Using a spatial and stage-structured invasion model to assess the spread of feral populations of transgenic oilseed rape. *Ecol. Modell*., 194, 141-149.

Gioria, M., Pyšek, P. & Moravcová, L. (2012). Soil seed banks in plant invasions: promoting species invasiveness and long-term impact on plant community dynamics. *Preslia* **84**, 327-350.

Greenman, J.V. & Benton, T.G. (2005) The impact of environmental fluctuations on structured discrete time population models: resonance, synchrony and threshold behaviour. *Theor. Popul. Biol.*, **68**, 217-235.

Halley, J.M. & Inchausti, P. (2004). The increasing importance of 1/*f*-noises as models of ecological variability. *FNL*, **4**, R1–R26.

Heino, M. & Sabadell, M. (2003), Influence of coloured noise on the extinction risk in structured population models. *Biol. Conserv.,* **110**, 315-325.

Heppell, S.S., Caswell, H. & Crowder, L.B. (2000). Life histories and elasticity patterns: perturbation analysis for species with minimal demographic data. *Ecology*, **81**, 654-665.

Jones, O.R., Scheuerlein, A., Salguero-Gómez, R., Camarda, C.G., Schaible, R., Casper, B.B., *et al*. (2014). Diversity of ageing across the tree of life. *Nature*, **505**, 169-173.

Jongejans, E., De Kroon, H., Tuljapurkar, S. & Shea, K. (2010). Plant populations track rather than buffer climate fluctuations. *Ecol. Lett.*, *13*, 736–743.

Koons, D.N., Iles, D.T., Schaub, M. & Caswell, H. (2016). A life-history perspective on the demographic drivers of structured population dynamics in changing environments. *Ecol. Lett.,* **19**, 1023-1031.

Koons, D.N., Metcalf, C.J. & Tuljapurkar, S. (2008). Evolution of delayed reproduction in uncertain environments: a life-history perspective. *Am. Nat.*, **172**, 797-805.

Koons, D.N., Pavard, S., Baudisch, A. & Metcalf, J.E. (2009). Is life-history buffering or lability adaptive in stochastic environments? *Oikos*, **118**, 972-980.

Laakso, J., Kaitala, V. & Ranta E. (2003). Non-linear biological responses to disturbance: consequences on population dynamics. *Ecol. Model.*, **162**, 247-258.

Levine, J.M. & Rees, M. (2004). Effects of temporal variability on rare plant persistence in annual systems. *Am. Nat.*, **164**, 350-363.

McDonald, J.L., Franco, M., Townley, S., Ezard, T.H., Jelbert, K. & Hodgson, D.J. (2017). Divergent demographic strategies of plants in variable environments. *Nature Ecol. Evol.*, **1**, 29.

Meijden, E.V., Klinkhamer, P.G., Jong, T.J. & Wijk, C.A. (1992). Meta- population dynamics of biennial plants: how to exploit temporary habitats. *Plant Biol.,* **41**, 249-270.

Metcalf, C.J., Ellner, S.P., Childs, D.Z., Salguero- Gómez, R., Merow, C., McMahon, S.M., *et al*. (2015). Statistical modelling of annual variation for inference on stochastic population dynamics using Integral Projection Models. *Methods Ecol. Evol.*, **6**, 1007-1017.

Metcalf, C.J., Horvitz, C.C., Tuljapurkar, S. & Clark, D.A. (2009). A time to grow and a time to die: a new way to analyze the dynamics of size, light, age, and death of tropical trees. *Ecology,* **90**, 2766-2778.

Metcalf, C.J. & Koons, D.N. (2007) Environmental uncertainty, autocorrelation and the evolution of survival. *Proc. R. Soc. Lond. B. Biol. Sci.*, 274, 2153-2160.

Morris, W.F., Altmann, J., Brockman, D.K., Cords, M., Fedigan, L.M., Pusey, A.E., *et al*. (2011). Low demographic variability in wild primate populations: fitness impacts of variation, covariation, and serial correlation in vital rates. *Am. Nat.,* **177**, E14-E28.

Morris, W.F. & Doak, D.F. (2004). Buffering of life histories against environmental stochasticity: accounting for a spurious correlation between the variabilities of vital rates and their contributions to fitness. *Am. Nat.,* **163**, 579-590.

Morris, W.F., Pfister, C.A., Tuliapurkar, S., Haridas, C.V., Boggs, C.L., Boyce, M.S., *et al.* (2008). Longevity can buffer plant and animal populations against changing climatic variability. *Ecology,* **89**, 19–25.

Morris, W.F., Tuljapurkar, S., Haridas, C.V., Menges, E.S., Horvitz, C.C. & Pfister, C.A. (2006). Sensitivity of the population growth rate to demographic variability within and between phases of the disturbance cycle. *Ecol. Lett.*, **9**, 1331-1341.

Nadeau, C.P., Urban, M.C. & Bridle, J.R. (2016). Coarse climate change projections for species living in a fine-scaled world. *Global Change Biol.*, **23**, 12-24.

Orzack, S.H. (1985) Population dynamics in variable environments. V. The genetics of homeostasis revisited. *Am. Nat.*, **4**, 550-72.

Post, E., Forchhammer, M.C., Bret-Harte, M.S., Callaghan, T.V., Christensen, T.R., Elberling, B., *et al*. (2009). Ecological dynamics across the Arctic associated with recent climate change. *Science*, **325**, 1355-1358.

Revell, L.J. (2012). phytools: An R package for phylogenetic comparative biology (and other things). *Methods Ecol. Evol.,* **3,** 217–223.

527 Ruokolainen, L., Linden, A., Kaitala, V. & Fowler, M.S. (2009). Ecological and evolutionary
528 dynamics under coloured environmental variation. *Trends in Ecol. Evol.*, **24**, 555-563.

529 Sæther, B.E., Coulson, T., Grøtan, V., Engen, S., Altwegg, R., Armitage, K.B., *et al*. (2013).
530 How life history influences population dynamics in fluctuating environments. *Am. Nat.,* **182***,*
531 743-759.

532 Salguero-Gómez, R. (2017). Applications of the fast–slow continuum and reproductive strategy
533 framework of plant life histories. *New Phytol*., **213**, 1618–1624.

534 Salguero-Gómez, R., Jones, O.R., Archer, C.R., Buckley, Y.M., Che-Castaldo, J., Caswell, H., *et*
535 *al.* (2015). The COMPADRE Plant Matrix Database: an open online repository for plant
536 demography. *J. Ecol.*, **103**, 202-18.

537 Salguero-Gómez, R., Jones, O.R., Archer, C.R., Bein, C., Buhr, H., Farack, C., *et al.* (2016a).
538 COMADRE: a global data base of animal demography. *J. Anim. Ecol.*, **85**, 371-384.

539 Salguero-Gómez, R., Jones, O.R., Jongejans, E., Blomberg, S.P., Hodgson, D.J., Mbeau-Ache,
540 C., *et al*. (2016b). Fast–slow continuum and reproductive strategies structure plant life-history
541 variation worldwide. *Proc. Natl. Acad. Sci.*, **113**, 230-235.

542 Schiesari, L. & O'Connor, M.B. (2013). Diapause: delaying the developmental clock in response
543 to a changing environment. *Curr. Top. Dev. Biol.,* **105**, 213–246.

544 Smallegange, I.M., Deere, J.A. & Coulson, T. (2014). Correlative changes in life-history
545 variables in response to environmental change in a model organism. *Am. Nat.*, **183**, 784-797.

546 Stearns, S.C. (1992). *The Evolution of Life Histories*. Oxford University Press, Oxford, pp. 247.

547 Steele, J.H. (1985). A comparison of terrestrial and marine ecological systems. *Nature*, **313**, 355-
548 358.

549 Stige, L.C., Chan, K.S., Zhang, Z., Frank, D. & Stenseth, N.C. (2007). Thousand-year-long
550 Chinese time series reveals climatic forcing of decadal locust dynamics. *Proc. Natl. Acad. Sci.*,
551 104, 16188-16193.

552 Tuljapurkar, S. (1990). *Population Dynamics in Variable Environments*. Springer, Berlin.

553 Tuljapurkar, S. (1982). Population dynamics in variable environments. II. Correlated
554 environments, sensitivity analysis and dynamics. *Theor. Popul. Biol.*, **21**, 114-140.

555 Tuljapurkar, S. & Haridas, C.V. (2006). Temporal autocorrelation and stochastic population
556 growth. *Ecol. Lett.*, **9**, 327-37.

557 Tuljapurkar, S., Horvitz, C.C. & Pascarella, J.B. (2003). The many growth rates and elasticities
558 of populations in random environments. *Am. Nat.,* **162**, 489-502.

559 Turner, M.G. (2010). Disturbance and landscape dynamics in a changing world. *Ecology*. **91**,
560 2833-2849.

561 Uller, T. (2008). Developmental plasticity and the evolution of parental effects. *Trends Ecol.*
562 *Evol*., **23**, 432-438.

563 Vasseur, D.A. & Yodzis, P. (2004). The color of environmental noise. *Ecology*, **85**, 1146-1152.

564

565 **SUPPORTING INFORMATION**

Additional Supporting Information may be downloaded via the online version of this article at Wiley Online Library (www.ecologyletters.com).

The data supporting the results of the study can be found on Dryad doi:10.5061/dryad.d851q.

As a service to our authors and readers, this journal provides supporting information supplied by the authors. Such materials are peer-reviewed and may be re-organized for online delivery, but are not copy-edited or typeset. Technical support issues arising from supporting information (other than missing files) should be addressed to the authors.

Table 1 Across simulations of vital-rate variation (*i*), sensitivity of the stochastic growth rate, log λ_s, to temporal autocorrelation (S^{v_1}) is affected by simulation parameters (CV and *f*) and differs between vital rates, life histories (defined by PCA scores in Figure 2; see also Table S2.1), and major habitat types. S^{v_1} also differ among habitat types when observed vital-rate covariation is modeled (simulating only *f*; *ii*). Parameter estimates from the most parsimonious GAM models are shown (see Appendix S3 for all models considered and details on parameters). Models fit at CV = 0.5 and *f* = 0.65 are indicated by arrows.

	Response variable	Explanatory variables	Best model	% S^{v_1} variation explained
(*i*) Simulated CV	$\log(S^{v_1})$	*f, CV*	$-8.30_{(0.08)} + 1.77_{(0.05)}CV_{0.5} + 2.85_{(0.05)}CV_{0.8} - 0.21_{(0.04)}f_{0.65}$ + ***s*(MatDim $_{df:6.3}$) + *s*(population $_{df:391.1}$)**	41.8
	$\log(S^{v_1})$ ➔ $CV_{0.5}$; $f_{0.65}$	*vital rate, PCA 1, PCA 2*	$-6.89_{(0.27)} + 1.15_{(0.28)}$Survival PR + $0.5_{(0.29)}$ Survival R + $1.1_{(0.29)}$Transitions PR + $0.11_{(0.30)}$Transitions R – $2.17_{(0.77)}$Reproduction P – $1.79_{(0.29)}$Reproduction PR + ***te*(PCA 1, PCA 2, Survival P $_{df:3.0}$) + *te*(PCA 1, PCA 2, Survival PR $_{df:7.2}$) + *te*(PCA 1, PCA 2, Survival R $_{df:3.0}$) + *te*(PCA 1, PCA 2, Transitions PR $_{df:6.0}$) + *te*(PCA 1, PCA 2, Transitions R $_{df:6.4}$) + *te*(PCA 1, PCA 2, Reproduction P $_{df:6.4}$) + *te*(PCA 1, PCA 2, Reproduction PR $_{df:6.1}$) + *s*(MatDim $_{df:6.3}$) + *s*(population $_{df:50.8}$)**	56.3

	$\log(S^{v_1})$ ➔ $CV_{0.5}$; $f_{0.65}$	*vital rate, habitat, PCA 1, PCA 2*	$-4.55_{(0.24)}$ - $0.30_{(0.09)}$Transitions – $3.62_{(0.09)}$Reproduction - $0.19_{(0.23)}$Temperate – $0.02_{(0.24)}$Tropical&Subtropical – $0.30_{(0.27)}$Arid + $0.04_{(0.5)}$Aquatic + ***te*(PCA 1, PCA 2, Survival** $_{\mathbf{df:6.1}}$**)** + ***te*(PCA 1, PCA 2, Transitions** $_{\mathbf{df:4.5}}$**)** + ***te*(PCA 1, PCA 2, Reproduction** $_{\mathbf{df:13.2}}$**)** + *te*(PCA 1, PCA 2, Alpine&Arctic $_{df:2.6}$) + ***te*(PCA 1, PCA 2, Temperate** $_{\mathbf{df:12.1}}$**)** + *te*(PCA 1, PCA 2, Tropical&Subtropical $_{df:2.6}$) + ***te*(PCA 1, PCA 2, Arid** $_{\mathbf{df:5.5}}$**)** + ***te*(PCA 1, PCA 2, Aquatic** $_{\mathbf{df:4.8}}$**)** + ***s*(MatDim** $_{\mathbf{df:3.0}}$**)**	72.8
***(ii)* Observed CV**	$\log(S^{v_1})$	*f*	***s*(MatDim** $_{\mathbf{df:0.3}}$**)**	39.4
	$\log(S^{v_1})$ ➔ $f_{0.65}$	*habitat, PCA 1, PCA 2*	$-6.44_{(0.19)} – 0.76_{(0.31)}$other + ***te*(PCA 1, PCA 2,Temperate** $_{\mathbf{df:1.9}}$**)** + ***te*(PCA 1, PCA 2,other** $_{\mathbf{df:1.0}}$**)**	51.7

CV (categorical covariate with values 0.2, 0.5, or 0.8) – coefficient of variation used to perturb vital-rate classes (P)propagules, Pre-reproductive (PR), and (R)eproductive; *f* – frequency of the good environmental state; MatDim/populations – dimension of the matrix population model and populations used in the study, respectively (fitted as nested random effects); Functions $te(x_{df})$ and $s(x_{df})$ are the tensor product and spline smoothing functions of x, respectively, with the given degrees of freedom *df*. Significant smoothing terms are in bold.

FIGURE LEGENDS

Figure 1 Simulations to test patterns of sensitivity of the stochastic growth rate, log λ_s, to temporal autocorrelation across life histories. From each matrix population model (MPM), obtained from COMADRE/COMPADRE, we extracted stage/age-specific vital rates as shown in (a) for survival (σ_2) of the second stage of an example MPM. We then perturbed each vital rate as a function of different coefficients of variation (CV) to obtain distributions of a vital rate above and below its average value (orange) and assembled MPMs for good and bad environmental states (b). Lastly, we used a Markov chain defined by the frequency of the good state (*f*) and autocorrelation coefficient (v_1) to create environmental sequences (*n* time steps) as shown by two examples in (c). We then simulated stochastic population dynamics where at each iteration *t* the environment was associated with one representative MPM (d). Gray boxes show analysis outputs; $\gamma/\rho/\varphi$ - stage-specific progression/retrogression/reproduction, respectively.

Figure 2 Life histories of study species' populations (points) are characterized by life-history traits representing the pace of life (fast-slow continuum) and lifetime reproduction (reproductive strategies). To characterize life histories, a phylogenetically-informed PCA was performed on five traits: generation time (T), age at sexual maturity (L_α), sexual reproduction (ϕ), iteroparity (S), and net reproductive rate (R_o). Arrow lengths are proportional to the loadings of each trait onto the two axes. Red points show populations with propagule (P) stages. Point sizes are proportional to the sensitivity of the stochastic population growth rate to temporal autocorrelation, S^{v_1}, summed across all vital rates (for simulations at CV = 0.5 and f = 0.65). Locations along the axes of some populations for which the effect of temporal autocorrelation on population dynamics has been assessed are shown; populations are colored based on relatively low (< 25th percentile; grey) and high (> 50th percentile; black) S^{v_1}.

Figure 3 Fast life histories (along PCA 1) across reproductive strategies (along PCA 2) generally show highest sensitivities of the stochastic growth rate, log λ_s, to temporal autocorrelation (S^{v_1}). Raster plots show predictions of S^{v_1} across the two PCA axes after perturbing various classes of vital rates across all habitats (a) and for five different habitat types (b). In (b), vital-rate classes include survival (S), stage/age transitions (T), and reproduction (R). Predictions were limited to the range of observed PCA scores. Number of vital-rate samples in each habitat are shown in parentheses. Points are proportional to raw S^{v_1} obtained from simulations. The results of vital-rate perturbations at CV = 0.5 and f = 0.65 are shown here (see Appendix S1 in Supporting Information for all results and Table 1 for significance of predictions). Locations along the axes of example populations discussed in the main text are shown.

Figure 4 Empirical patterns of the sensitivities of the stochastic growth rate, log λ_s, to temporal autocorrelation (S^{v_1}) validate simulations. (a) Among 109 population for which observed vital-rate co-variance was used to define good and bad environmental states, fast life histories (along PCA 1) across reproductive strategies (along PCA 2) show highest S^{v_1} in temperate and other habitat types. (b) S^{v_1} obtained from simulations (a) for 13 species with the longest time-series data (≥ 10 annual matrix population models) are significantly correlated, on a log scale, (R^2 = 0.60; $p < 0.05$) with relative deviance explained by first-order autoregressive vital-rate models for the same populations (deviances, $\overline{D^2}$, shown are averaged over vital-rate models). (b) For the 454 populations used to simulate S^{v_1}, log(S^{v_1}; grey points) differ among published studies that determined v_1 to be an important component of population dynamics (yes) and ones that did not (no).

632 **FIGURE 1**

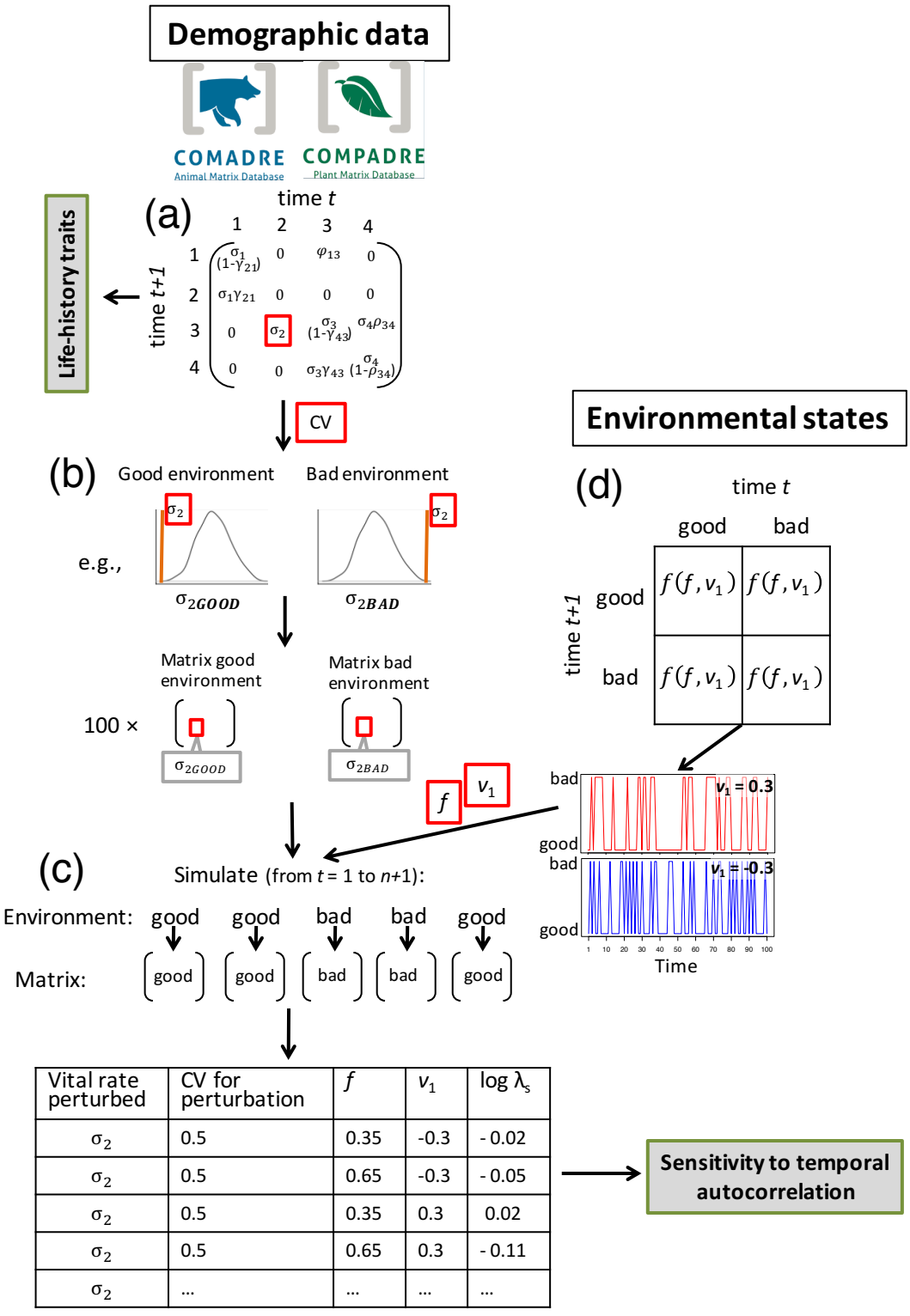

Vital rate perturbed	CV for perturbation	f	v_1	log λ_s
σ_2	0.5	0.35	-0.3	- 0.02
σ_2	0.5	0.65	-0.3	- 0.05
σ_2	0.5	0.35	0.3	0.02
σ_2	0.5	0.65	0.3	- 0.11
σ_2	...	...	...	...

633

FIGURE 2

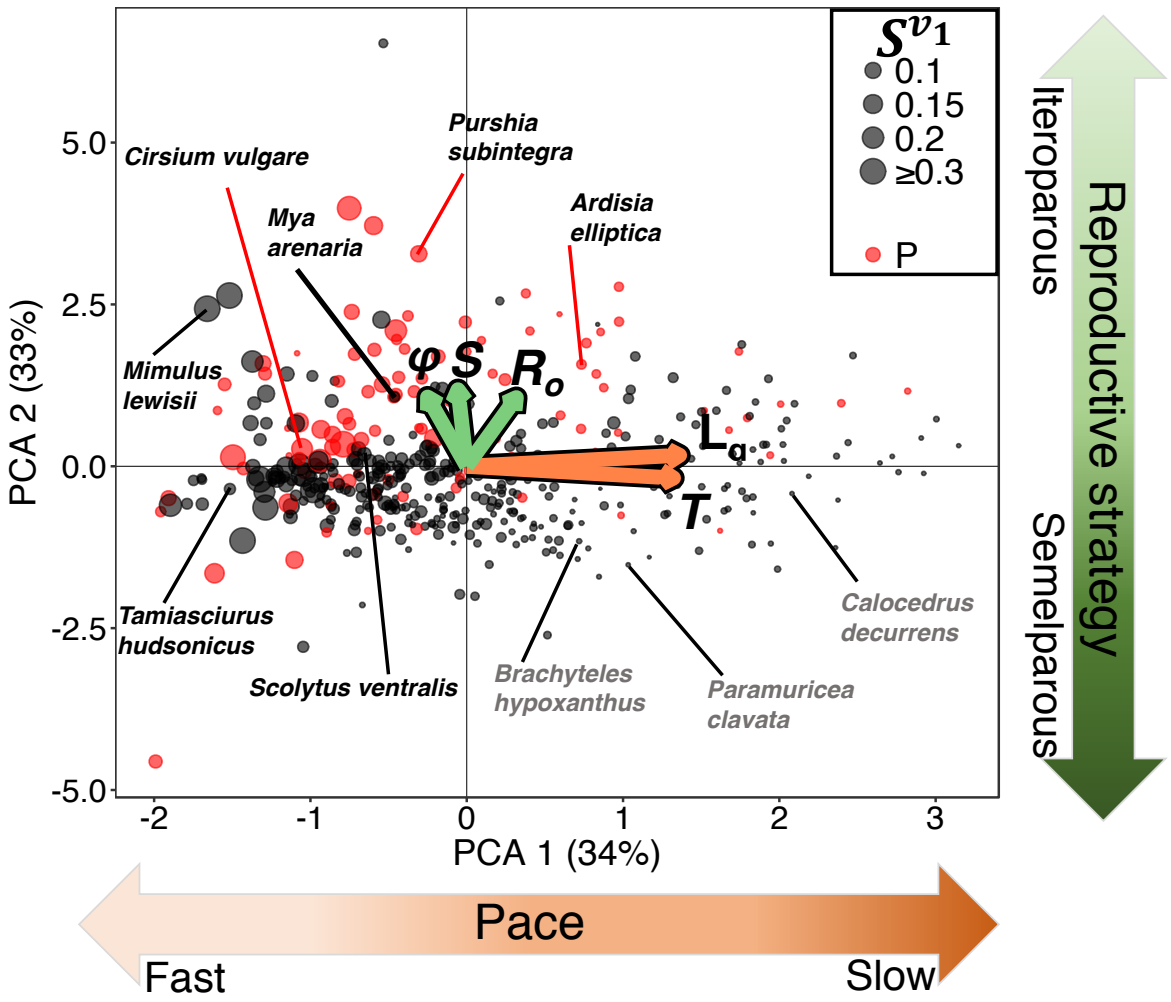
S^{v_1}
0.1
0.15
0.2
≥0.3
P
Cirsium vulgare
Purshia subintegra
Mya arenaria
Ardisia elliptica
Mimulus lewisii
φ
S
R_o
L_q
T
Tamiasciurus hudsonicus
Scolytus ventralis
Brachyteles hypoxanthus
Paramuricea clavata
Calocedrus decurrens
PCA 2 (33%)
PCA 1 (34%)
5.0
2.5
0.0
-2.5
-5.0
-2
-1
0
1
2
3
Iteroparous
Semelparous
Reproductive strategy
Pace
Fast
Slow

642 **FIGURE 3**

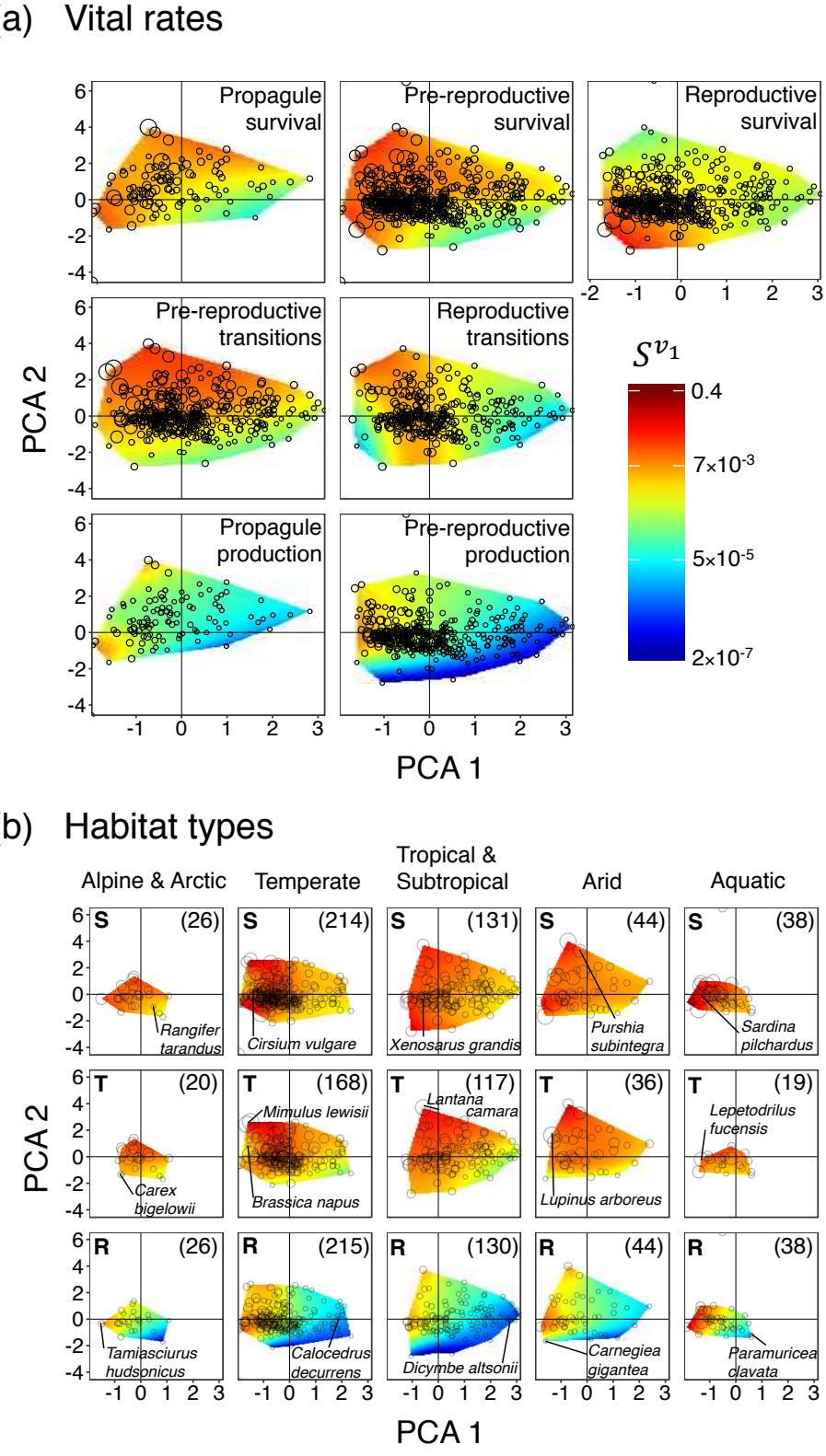

643

644 **FIGURE 4**

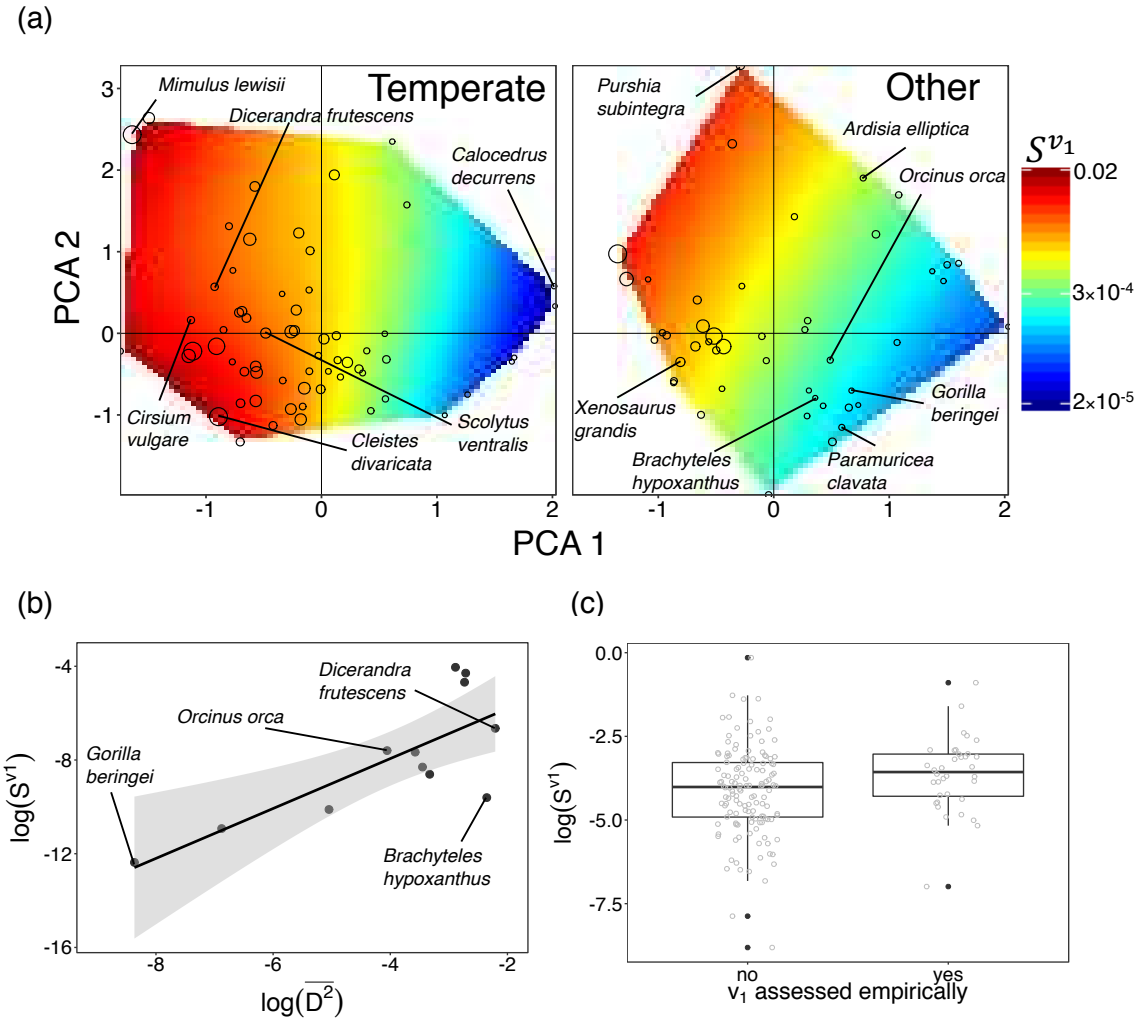

645

646

647